Technical Report No. 20

2

SACLANT ASW
RESEARCH CENTER

FREQUENCY DEVIATION INDICATOR

by

H.A.J. RYNJA

20 November 1963

NATO — VIALE SAN BARTOLOMEO, 92
LA SPEZIA, ITALY

This document is released to a NATO Government at the direction of the SACLANTCEN subject to the following conditions:

1. The recipient NATO Government agrees to use its best endeavours to ensure that the information herein disclosed, whether or not it bears a security classification, is not dealt with in any manner (a) contrary to the intent of the provisions of the Charter of the Centre, or (b) prejudicial to the rights of the owner thereof to obtain patent, copyright, or other like statutory protection therefor.

2. If the technical information was originally released to the Centre by a NATO Government subject to restrictions clearly marked on this document the recipient NATO Government agrees to use its best endeavours to abide by the terms of the restrictions so imposed by the releasing Government.

TECHNICAL REPORT 20

SACLANT ASW RESEARCH CENTER
Viale San Bartolomeo 92
La Spezia, Italy

FREQUENCY DEVIATION INDICATOR

By

H. A. J. Rynja

20 November 1963

APPROVED FOR DISTRIBUTION

John M. Ide
JOHN M. IDE
Director

FREQUENCY DEVIATION INDICATOR

By

H. A. J. Rynja

Summary

A new type of discriminator has been developed to measure the frequency variation of electrical signals; it has the special feature to indicate without any delay the difference between the signal frequency and some fixed reference frequency.

The discriminator consists of two different parallel, frequency sensitive, networks, the outputs of which are always either in phase or in phase opposition but have different amplitudes. On a CRT screen these two voltages produce a line; the length of the line gives the amplitude and its direction gives the frequency of the original signal. By a proper choice of some circuit parameters, the indication can be made linear with the frequency within a relatively large frequency band. Between the limits of noise and overload of the amplifiers, the signal amplitude has no influence on the indicated angle.

The same networks can be used to construct a simple discriminator that produces a DC voltage proportional to the frequency deviation as is done by FM demodulator circuits. Among the many applications of this discriminator this report describes the registration of the changes in the earth's magnetic field with the use of a Rubidium Vapour Magnetometer and the recording of the variations in the sound velocity in sea water using a Daystrom Sound Velocity Meter.

INTRODUCTION

The indication of the frequency variations of an electrical signal requires a frequency sensitive instrument. There are many circuits that give a response on frequency variations, called "discriminators," well known for demodulation of FM signals. Most of the discriminators are composed of resonant circuits or delay lines followed by a rectifier. Due to the delay line, or to the DC filter following the rectifier, all these circuits inhibit a certain time constant. Furthermore, the amplitude of the original signal sometimes influences, more or less, the output voltage so that an amplitude limiter is needed to reduce the variations in signal voltage. However, limiters are only effective in a restricted frequency band; they have a certain time constant also, and thoy never reduce the signal variations to zero. Therefore, when the frequency of short signal pulses or amplitude modulated signals has to be measured, most of the known discriminator circuits are unable to give a clear and precise indication.

The instrument described gives a representation of the frequency deviation Δf_o from a certain frequency f_o of a sinusoidal electric signal. The indication is independent of the amplitude of the signal and is without any time delay. However, it is well known that the frequency of an amplitude modulated signal cannot be given by only one number; instead, it is represented by a certain frequency band depending on the waveform of the modulation. It is clear that this uncertainty in the numerical value of the frequency will be recorded also.

The indication appears on an oscilloscope screen as the angle of inclination ϕ of a straight line. It can be proved that a proper choice of various circuit parameters results in a symmetric frequency deviation scale.

This last fact is important when the frequency deviations are of the same magnitude as the mean frequency. Many frequency selective networks give a response that is a symmetrical on a logarithmic frequency scale, so that the same output in absolute value will be found for any pair of frequencies pf_o and $\frac{f_o}{p}$. However, the linear symmetry of the discriminator described here means that the same angles $+\phi$ and $-\phi$ are indicating the frequencies of $f_o + \Delta f_o$ and $f_o - \Delta f_o$.

If a time-record of the frequency deviations is desired, a phase sensitive detector can be added to the circuit, giving a DC voltage more or less proportional to the frequency deviation Δf_o. This can be recorded on any DC paper recorder. In this case, a limiter is needed also, and the instrument offers no advantage over other conventional discriminators which have a certain time constant. However, it can be said, that the circuit is very simple, and a relatively large frequency band (0 to 2 f_o and even higher) can be covered. Also, the same type of circuit can be designed for a very high sensitivity in a small bandwidth.

PART I

OSCILLOSCOPE DISPLAY

1.1 Principle of Operation

The basic principle of the discriminator is the comparison of two signals that are produced by processing the original signal through two different frequency sensitive networks. These networks are so designed that the two signals they produce are either in phase or in phase opposition for all frequencies. These two signals are indicated respectively by $\bar{a}$ and $\bar{c}$. Figure 1 gives the block diagram of the discriminator; the original signal is indicated by $\bar{e}$.

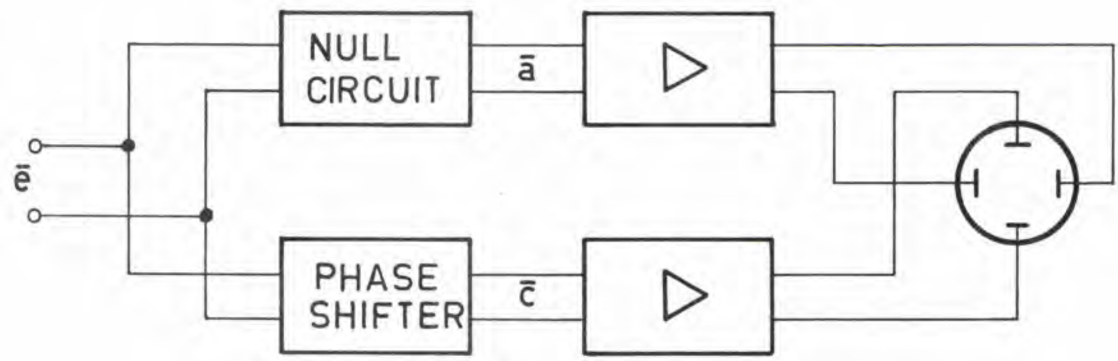

Fig. 1 Basic Block Diagram of Discriminator

The circuit that produces the signal $\bar{a}$ is a "null circuit": at the frequency f_o the amplitude of $\bar{a}$ goes through zero while the phase difference between $\bar{a}$ and $\bar{e}$ jumps from 90^o to 270^o. The "$\bar{c}$-circuit" is a phase-shifter that produces a phase shift of 90^o at the frequency f_o.

When the signals $\bar{a}$ and $\bar{c}$ are applied to the horizontal and vertical deflection systems of an oscilloscope, a straight line appears on the screen; the position of the line is determined by the amplitude ratio of $\bar{a}$ and $\bar{c}$. In the following paragraphs, an analysis will be given for different $\bar{a}$- and $\bar{c}$-circuits in order to find the conditions for which the slope ϕ of the trace on the CRT-screen is linearly proportional to the frequency deviation Δf_o.

1.2 The $\bar{a}$-circuit

The $\bar{a}$-circuit is a bridge that gives complete signal extinction for one frequency; this frequency is the central frequency f_o. For the purpose of generalization of the equations, the relative frequency β will be introduced as

$$\beta = \frac{f}{f_o} = \frac{\omega}{\omega_o} \tag{1}$$

where f and ω are the frequency and the angular frequency of the original signal respectively.

1.2.1 <u>The Wien - Bridge</u>. Figure 2 gives the circuit diagram for the Wien-Bridge. The factor n in this circuit may have any value between 0 and ∞. This fact gives the desired flexibility to the circuit in order to obtain a symmetric frequency shift indication by a proper choice of its value. (This will be discussed in Sect. 1.6). The condition to have zero output at the frequency f_o for this circuit is

$$\omega_o R_1 C_1 = 1 \tag{2}$$

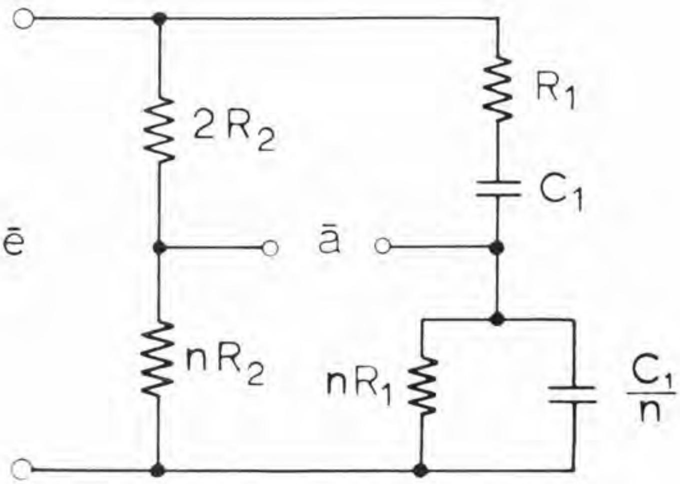

Fig. 2 Wien Bridge as Null Circuit

The value of R_2 can be chosen arbitrarily.

The output voltage $\bar{a}$ of this circuit is given by

$$\frac{\bar{a}}{\bar{e}} = \frac{n}{n+2} \cdot \frac{-1}{1 - j \frac{\beta}{\beta^2 - 1} (n+2)} \tag{3}$$

with a phase angle α given by

$$\operatorname{tg} \alpha = (n+2) \frac{\beta}{\beta^2 - 1} \tag{4}$$

The vector diagram of $\bar{a}$ in the complex plane is given by Fig. 3.

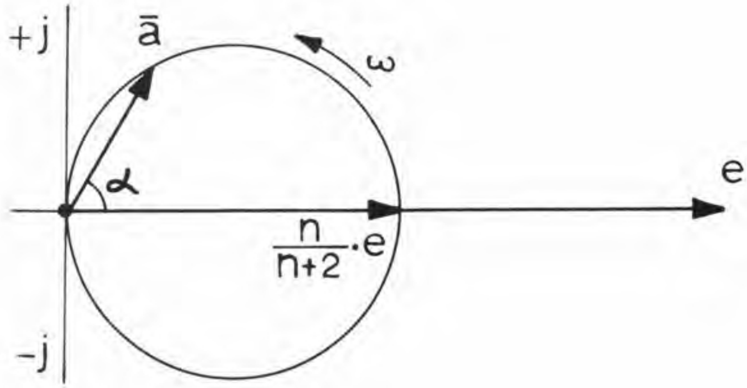

Fig. 3 Vector Diagram of the Wien Bridge

1.2.2 <u>The Bridged-T</u>. Figure 4 shows the circuit diagram for the Bridged-T.

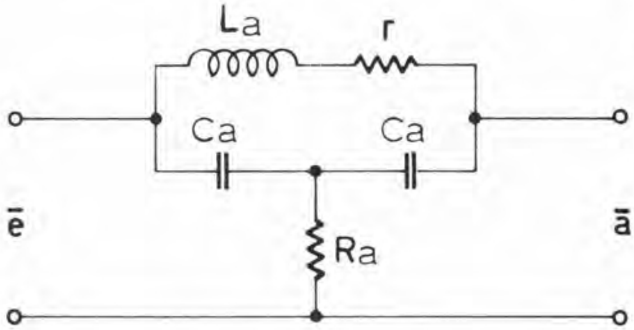

Fig. 4 The Bridged-T-Null Circuit

The conditions for this circuit to give an output zero at the angular frequency ω_o are

$$\omega_o^2 L_a C_a = 2 \tag{5}$$

and

$$L_a = 2r R_a C_a \tag{6}$$

By introducing the quality factor Q_a of the coil L_a as

$$Q_a = \frac{\omega_o L_a}{r} \tag{7}$$

and the relative frequency β from Eq. (1), the transfer function of the bridged-T is found to be

$$\frac{\bar{a}}{\bar{e}} = \frac{1}{1 - j\frac{\beta}{\beta^2 - 1} \cdot \frac{2}{Q_a}} \tag{8}$$

The phase angle α between $\bar{a}$ and $\bar{e}$ is given by

$$\text{tg}\ \alpha = \frac{2}{Q_a} \cdot \frac{\beta}{\beta^2 - 1} \tag{9}$$

The vector diagram of $\bar{a}$ is given in Fig. 5.

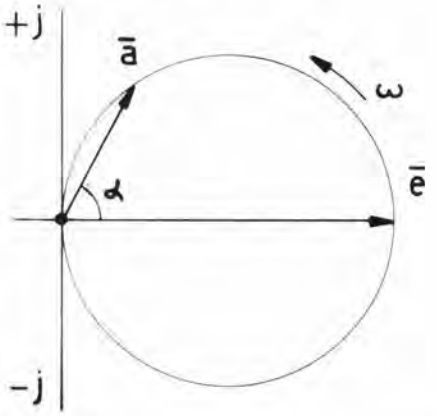

Fig. 5. Vector Diagram of the Bridged T

1.3 The $\bar{c}$-circuit

The $\bar{c}$-circuit is a phase shifter that must produce a phase shift of 90^o with respect to the original signal at the frequency f_o. For other frequencies, the phase angle, indicated by γ, should be equal to the phase angle α of the $\bar{a}$-circuits. There are several circuits that meet these conditions; the two most useful of these will be described here.

1.3.1 <u>The RC Phase Shifter.</u> Figure 6 gives the diagram of the RC Phase Shifter with k indicating a factor between 0 and 1. This factor is needed to obtain a complete phase-equality with one of the given $\bar{a}$-circuits. In this circuit the frequency, where $\omega R_3 C_3 = 1$, is not equal to f_o but differs from that frequency by a factor ϵ.

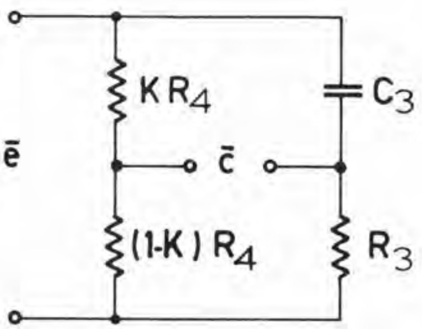

Fig. 6 The RC Phase Shifter

The factor ϵ can be defined as

$$\epsilon = \omega_o R_3 C_3 \tag{10}$$

The complex output voltage $\bar{c}$ is given by

$$\frac{\bar{c}}{\bar{e}} = \frac{1}{1 + j \epsilon \beta} - k \tag{11}$$

The phase angle γ between $\bar{c}$ and $\bar{e}$ is given by

$$\text{tg } \gamma = \frac{\epsilon \beta}{k(1 + \epsilon^2 \beta^2) - 1} \tag{12}$$

The vector diagram of $\bar{c}$ is given in Fig. 7.

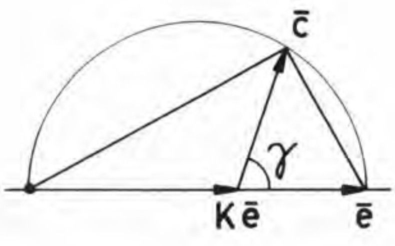

Fig. 7 Vector Diagram of the RC Phase Shifter

1.3.2 <u>The LC Phase Shifter</u>. Figure 8 gives the circuit diagram for the LC Phase Shifter.

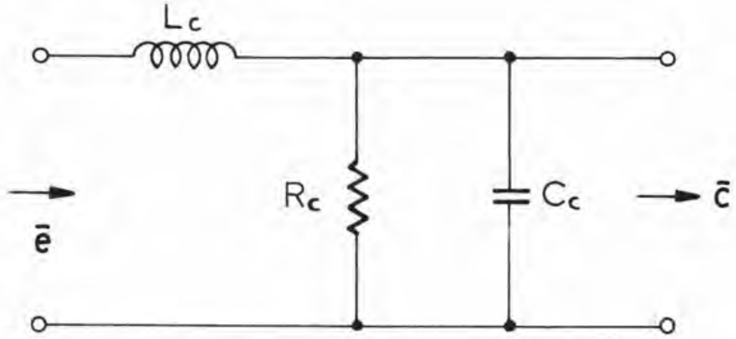

Fig. 8 The LC Phase Shifter

The condition for 90° phase shift at the frequency f_o is

$$\omega_o^2 \; L_c \, C_c \; = \; 1 \tag{13}$$

The quality factor Q_c of this circuit will be introduced as

$$Q_c = \omega_o \, R_c \, C_c \tag{14}$$

This factor can be used to obtain equal phase shift of this circuit with one of the $\bar{a}$-circuits.

The complex output voltage $\bar{c}$ is given by

$$\frac{\bar{c}}{\bar{e}} = \frac{1}{1 - \beta^2 + j \, \frac{\beta}{Q_c}} \tag{15}$$

The phase angle γ is given by

$$\operatorname{tg} \gamma = \frac{1}{Q_c} \cdot \frac{\beta}{\beta^2 - 1} \tag{16}$$

1.4 Condition for Equal Phase

To obtain a single line, and not an ellipse, on the oscilloscope screen, the two signals $\bar{a}$ and $\bar{c}$ should have a phase difference of 0° or 180° when they are applied to the horizontal and vertical deflection systems. This condition is covered by the equation

$$\operatorname{tg} \alpha = \operatorname{tg} \gamma \tag{17}$$

for all frequencies. With this equation, the variable parameters in the different $\bar{a}$ and $\bar{c}$-circuits can be solved, since they are the factors n, Q_a, k, ϵ, and Q_c. (Eqs. (4), (9), (12), and (16) refer).

1.5 Display

By feeding the signal $\bar{a}$ to the horizontal and $\bar{c}$ to the vertical amplifier of an oscilloscope, a straight line appears on the screen, which makes an angle ϕ with the vertical. With equal sensitivity of both channels this angle ϕ is given by

$$\operatorname{tg} \phi = \frac{\bar{a}}{\bar{c}} \tag{18}$$

Substituting the equations for $\bar{a}$ and $\bar{c}$ as functions of β, the inclination angle ϕ can be found as function of β. By a proper choice of one of the parameters mentioned above, this function can be given some symmetry and linearity as will be seen later in Section 1.6.

The following sections give some examples of useful combinations of $\bar{a}$ and $\bar{c}$ circuits as was shown in Fig. 1.

1.5.1 Combination of Wien Bridge and RC-Bridge. Equation (17) must be applied to Eqs. (4) and (12), giving

$$(n + 2) \frac{\beta}{\beta^2 - 1} = \frac{\epsilon \beta}{k(1 + \epsilon^2 \beta^2) - 1} \tag{19}$$

Solving this equation for all values of β yields

$$n = \frac{(\epsilon - 1)^2}{\epsilon} \tag{20}$$

$$k = \frac{1}{\epsilon^2 + 1} \tag{21}$$

For every chosen value of ϵ one value for n and k can be found, so that the circuits can be realized. The choice of ϵ allows some symmetry to be introduced.

Substituting (20) and (21) in (3) and (11) gives the values of $\bar{a}$ and $\bar{c}$ as functions of β. Substitution of these values in (18) gives

$$\text{tg } \phi = \frac{(\epsilon - 1)^2 (\beta^2 - 1)}{\epsilon^2 + \beta^2} \tag{22}$$

1.5.2 Combination of Bridged-T and RC-Bridge. Equations (9) and (12) have to be substituted in Eq. (17), which gives

$$\frac{2}{Q_a} \cdot \frac{\beta}{\beta^2 - 1} = \frac{\epsilon \beta}{k(1 + \epsilon^2 \beta^2) - 1} \tag{23}$$

Solving this equation for all values of β yields

$$Q_a = \frac{2 \epsilon}{\epsilon^2 + 1} \tag{24}$$

$$k = \frac{1}{\epsilon^2 + 1} \tag{25}$$

Substituting these values in (8) and (11), and substituting the latter equations in (18), gives

$$\mathrm{tg}\ \phi = \frac{(\epsilon^2 + 1)\ (\beta^2 - 1)}{\epsilon^2 + \beta^2} \tag{26}$$

In the same way as mentioned in Section 1.5.1, the factor ϵ is still free to give this function the desired linearity and symmetry.

1.5.3 Combination of Bridged-T and LC Phase Shifter. Here, the parameters can be solved by substitution of the functions (9) and (16) in Eq. (20) to give

$$\frac{2}{Q_a} \cdot \frac{\beta}{\beta^2 - 1} = \frac{1}{Q_c} \cdot \frac{\beta}{\beta^2 - 1} \tag{27}$$

with the solution

$$Q_a = 2\ Q_c \tag{28}$$

Substitution of Eqs. (8) and (15) in (18) gives, with (28)

$$\text{tg}\ \phi = 1 - \beta^2 \tag{29}$$

This function shows no parameter: it is independent from Q_a and Q_c. A plot of this function is given in Fig. 9, which shows the non-linearity of this type of frequency indicator.

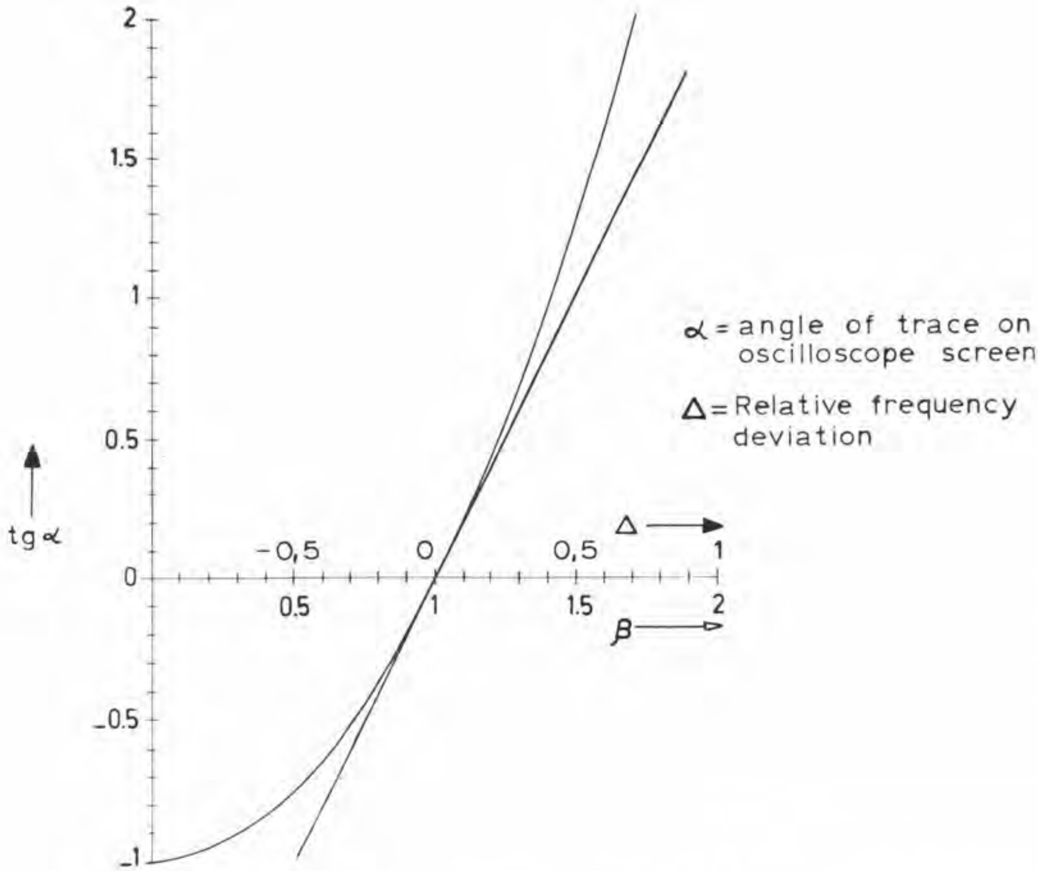

Fig. 9 Visual Display Response Curve of LC Discriminator

1.6 Symmetry

In order to find the right value for ϵ in the functions (22) and (26), the relative frequency deviation Δ will be introduced, defined as follows: the frequency f can be related to the central frequency f_o as

$$f = f_o + \Delta f_o \tag{30}$$

introducing Δ as

$$\Delta = \frac{\Delta f_o}{f_o} \tag{31}$$

Δ is a factor between -1 and +1, or sometimes even higher than +1. Equation (1) yields

$$\beta = 1 + \Delta \tag{32}$$

Now, the condition for symmetry will be satisfied as follows, when

$$\Delta = + \Delta_1, \qquad \mathrm{tg}\ \phi = + T$$

and, when (33)

$$\Delta = - \Delta_1, \qquad \mathrm{tg}\ \phi = - T$$

Applying this principle to the functions (22) and (26), ϵ can be solved to the value that gives symmetry to the ϕ vs. Δ curve.

It will be found for both functions that

$$\epsilon^2 = 3 - \Delta^2 \tag{34}$$

Obviously a complete symmetry for all values of Δ cannot be realized, as the required value for ϵ still depends on Δ. But, when $\Delta^2 \ll 3$, it will be found that

$$\epsilon \approx \sqrt{3} \tag{35}$$

The remaining unknown parameters in the circuits can now be solved from Eqs. (20), (21), (24), and (28)

$$\begin{aligned} n &= 0.31 \\ k &= 1/4 \\ Q_a &= 1/2 \sqrt{3} \\ Q_c &= 1/4 \sqrt{3} \end{aligned} \tag{36}$$

The curves giving the display angle on the oscilloscope screen versus the relative frequency deviation Δ for the different combinations of circuits can be drawn from Eqs. (22) and (26) substituting $\epsilon = \sqrt{3}$ and $\beta = 1 + \Delta$.

Referring to the combination of the Wien Bridge and the RC Bridge: Eq. (22)

$$\operatorname{tg} \phi = 0.536 \ \Delta \ \frac{\Delta + 2}{\Delta^2 + 2\Delta + 4} \tag{37}$$

Referring to the combination of the Bridged-T and the single RC-Bridge: Eq. (26)

$$\mathrm{tg}\,\phi = 4\,\Delta\,\frac{\Delta + 2}{\Delta^2 + 2\,\Delta + 4} \tag{38}$$

These functions are the same, apart from a constant factor that only influences the sensitivity of the indicator.

The general curve

$$\mathrm{tg}\,\phi = \frac{\Delta\,(\Delta + 2)}{\Delta^2 + 2\,\Delta + 4} \tag{39}$$

is drawn in Fig. 10, and shows the good linearity in the vicinity of $\Delta = 0$ compared to Fig. 9.

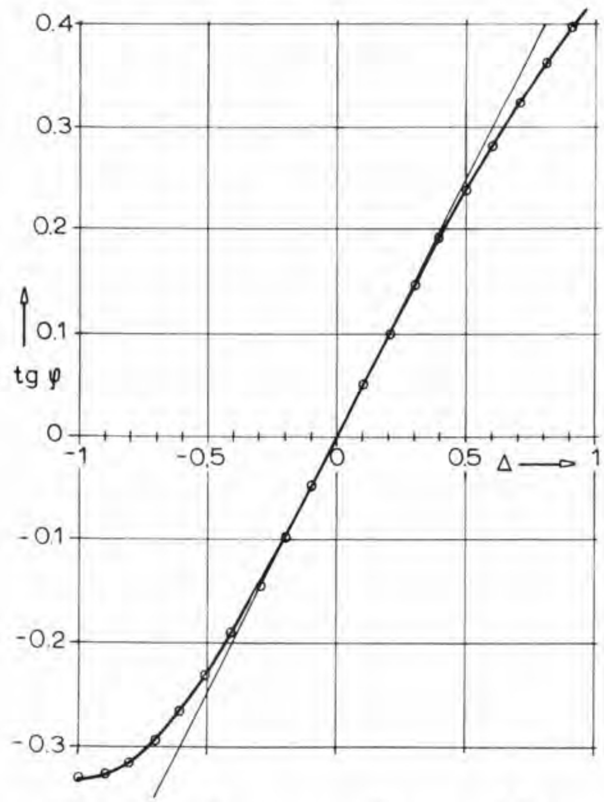

Fig. 10 Visual Display Response Curve of Symmetrified RC Discriminator

1.7 Conclusion

A symmetrical indication of frequency deviations as high as half the central frequency ($\Delta < 0.5$) can be obtained by combination of a "null-network" with a RC phase shifter. Indication is still possible for higher frequency deviations but the symmetry will be poor. The null-network can be composed only of resistors and capacitors.

The sensitivity of the indicator can be changed between wide limits by changing the gain of the amplifiers in the two channels.

When only weak signals are available in a noisy background and when the frequency deviations are relatively small, the Wien-Bridge will give no clear indication. In this case, the Bridged-T can be used in the $\bar{a}$-channel and the LC phase shifter in the $\bar{c}$-channel, both with high Q-values, bearing in mind Eq. (28) $Q_a = 2\,Q_c$. For small frequency changes ($\Delta < 0.1$), the symmetry of this type of discriminator will be good enough, as can be seen from Fig. 9.

PART 2

REGISTRATION ON A DC - RECORDER

2.1 Principles

The same circuits that are described in Part 1 can be used to construct a discriminator, which produces a DC voltage proportional (between certain limits) to the frequency deviation Δ similar to a FM demodulator.

2.1.1 <u>Division</u>. When the signal $\bar{a}$ is divided by the signal $\bar{c}$ with the aid of some electronic divider, a DC component will be obtained which is approximately proportional to the frequency deviation Δ and independent of the amplitude of the original signal. The same parameter values that are found in Part 1 will also give a symmetric frequency deviation scale in this case. However, the complexity of a 4-quadrant electronic divider is a great drawback for the practical use of this type of discriminator.

2.1.2 <u>Multiplication</u>. Electronic multiplication of the two signals $\bar{a}$ and $\bar{c}$ gives also a DC voltage, which is a monotone function of the frequency deviation Δ but it is also proportional to the square of the original signal voltage. An amplitude limiter is required to keep the input voltage $|\bar{e}|$ constant. A proper choice of the circuit parameters here leads also to a symmetrical frequency deviation scale. These factors must be the same as in Part 1 (see Eq. (36)) except for

$$\epsilon = 1/3 \quad \sqrt{3}$$

and

$$k = 3/4$$

Possible multipliers are:

1. Hall generator multiplier
2. Square law diode multiplier
3. Pentagrid converter tube multiplier, etc.

2.1.3 Rectification. The simplest way to obtain a frequency dependent DC voltage is to rectify the signal $|\bar{a}|$ with a phase sensitive detector, using the signal $\bar{c}$ only as a phase reference. The rectifier will produce a DC voltage proportional to $|\bar{a}|$ as long as $\bar{a}$ and $\bar{c}$ are in phase, and proportional to $-|\bar{a}|$ when $\bar{a}$ and $\bar{c}$ are in phase opposition. In order to obtain an output voltage at the discriminator that is dependent only on the frequency of the signal, an amplitude limiter is needed to reduce the amplitude variations of the original signal. Figure 11 gives the circuit diagram of a phase sensitive detector on which the balanced DC output voltage is indicated by D. In order to raise the voltage level of D, the resistors r, in series with the diodes, serve to increase the impedance of the conducting branch of the diode bridge.

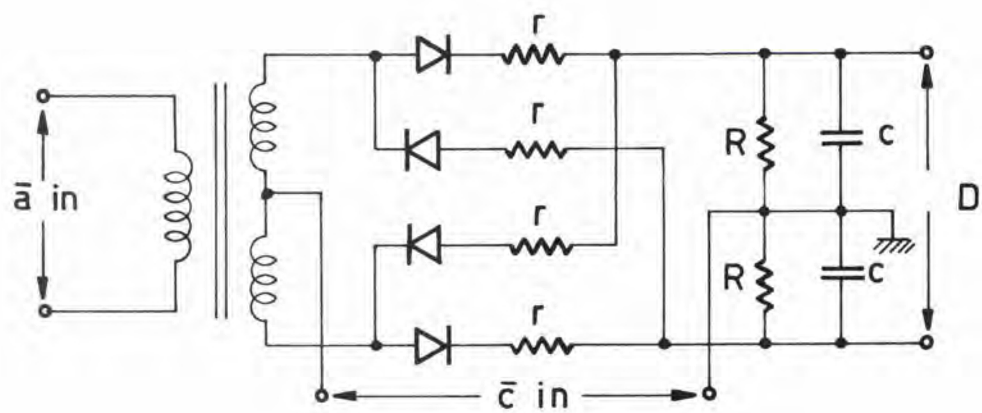

Fig. 11 Phase Sensitive Detector

2.2 Analysis of Discriminator with Rectifier

The principle mentioned in Section 2.1.3 will be considered more in detail. Figure 12 gives a block diagram of this type of discriminator.

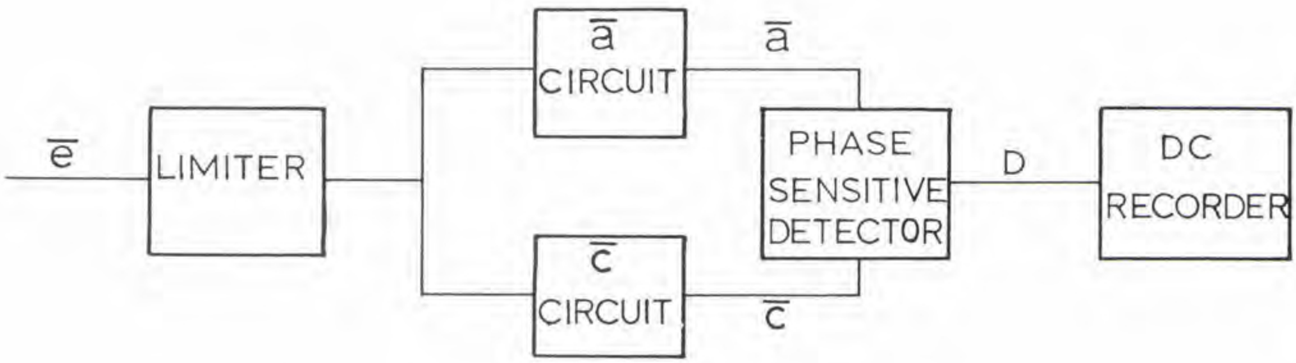

Fig. 12 Block Diagram of DC Discriminator

2.2.1 <u>Response Curve</u>. The output voltage D is proportional to $\pm\ |\bar{a}|$; the sign depends on the phase between $\bar{a}$ and $\bar{c}$. The curve for D, as a function of the relative frequency deviation Δ, can be derived from Eqs. (3) or (8), depending on the type of $\bar{a}$-circuit that has been chosen. As an example, Eq. (8) has been taken, substituting

$$\bar{e} = 1, \quad Q_a = 1$$

and

$$\beta = \Delta + 1$$

Hence

$$\bar{a} = \frac{1}{1 - \frac{2j}{\Delta} \quad \frac{\Delta + 1}{\Delta + 2}} \tag{40}$$

The curve $D = \pm \left| \bar{a} \right|$ is drawn in Fig. 13.

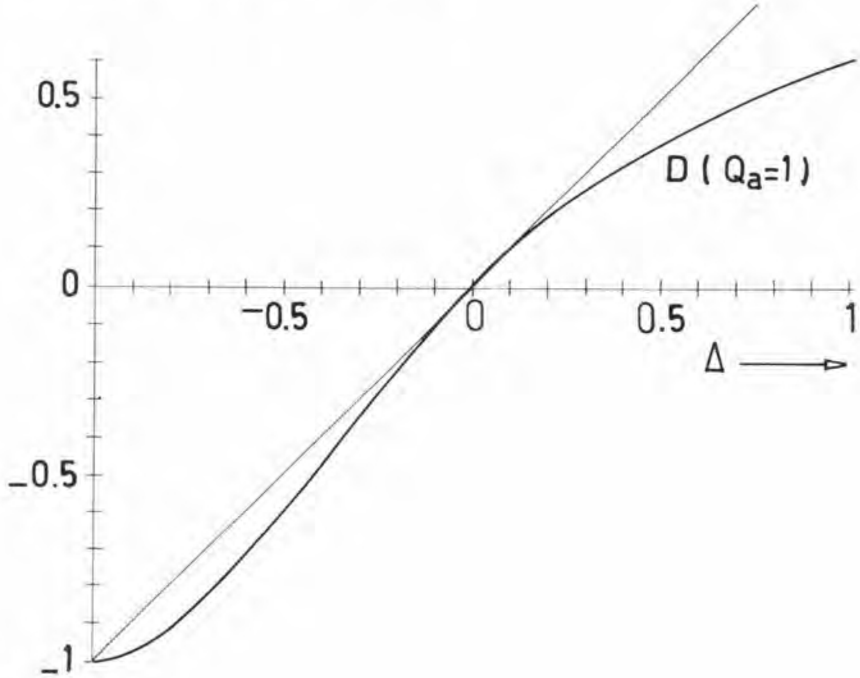

Fig. 13 Response Curve of Discriminator: DC Voltage at Recorder as a Function of Δ

Other curves for other values of Q_a, or derived from Eq. (3) with different values of the parameter n, have all about the same general shape, but the slopes at $\Delta = 0$ are different.

2.2.2 Sensitivity. The sensitivity of the discriminator is defined by the ratio between the output voltage D and the relative frequency deviation Δ as

$$S = \frac{D}{\Delta} \tag{41}$$

As the output voltage D is proportional to $\left| \bar{a} \right|$ (or $-\left| \bar{a} \right|$), Eq. (41) can be written as

$$S = \left| \frac{\bar{a}}{\Delta} \right| \tag{42}$$

Solving this equation for $\Delta \to 0$ gives the sensitivity S_o at this point of the curve. The input signal $\bar{e}$ of the discriminator is assumed to be 1 v.

For the Wien-Bridge, the sensitivity can be found from Eq. (3)

$$S_o = \frac{2n}{(n+2)^2} \tag{43}$$

For the Bridged-T, Eq. (8) has to be taken, giving

$$S_o = Q_a \tag{44}$$

The maximum of Eq. (43) will be found when $n = 2$ and has the value $S_{omax} = 0.25$. Equation (44), however, shows no maximum but increases at any value that can be given to Q_a. Therefore, the Bridged-T can definitely give a higher sensitivity to the discriminator than the Wien-Bridge circuit.*

---

*For this reason, the Wien-Bridge will be used only for the CRT display indicator of Part 1 and in those cases where the use of coils is prohibitive or undesirable for some reason, as for instance:

1. The inductance of the coils is temperature dependent; a change in temperature will cause a shift of the center frequency. The error in indication, arising in this way, increases with increasing sensitivity.

2. The inductance of the coils is also dependent on the level of the signal above a certain value. This also causes a shift in central frequency and distortion at higher signal amplitudes.

3. The LC-circuits are more expensive, heavier, and bigger than the RC-circuits.

2.2.3 Impedance of $\bar{a}$ and $\bar{c}$-circuits. When two networks are fed in parallel from one source, it is advisable, from the point of view of energy distribution, to have the impedance of the two networks equal. When feeding the Bridged-T and the LC phase shifter in parallel from the same amplifier, their impedance can be equalized by a proper choice of the ratio $\frac{L_c}{L_a}$. (Ref. Figs. 4 and 8).

The impedance of the Bridged-T at the frequency ω_o is:

$$\left| \bar{Z}_{ao} \right| = \frac{\omega_o L_a}{2} \sqrt{Q_a^2 + 1} \tag{45}$$

The impedance of the LC phase shifter at the same frequency is

$$\left| Z_{co} \right| = \frac{\omega_o L_c}{\sqrt{Q_c^2 + 1}} \tag{46}$$

These impedances are equal when

$$\frac{L_c}{L_a} = \frac{Q_a^2 + 2}{4} \tag{47}$$

since $Q_a = 2Q_c$. (Eq. 28)

Because the ratio of L_c and L_a does not otherwise influence the response curve of this discriminator, the choice of their values is free. Hence, Eq. (47) can be helpful for the final design of the circuits.

2.3 Extension of the Frequency Range

The center frequency of the discriminator has a fixed value that cannot easily be changed. When the frequency deviation from another mean value has to be recorded, the other mean frequency has to be converted to the center frequency of the discriminator.

Because of its ability to suppress the original signals and to produce only modulation products, out of which the fundamental mode can be filtered easily, a ring modulator may be used as converter.

The unknown frequency f_1 will be mixed with the frequency of a signal generator $f_1 \pm f_o$ to produce the discriminator center frequency f_o. It is important that the frequency of the signal generator is constant compared with the frequency of the signal to be measured. A crystal controlled oscillator can be used if needed.

A block diagram of the complete discriminator is given in Fig. 14.

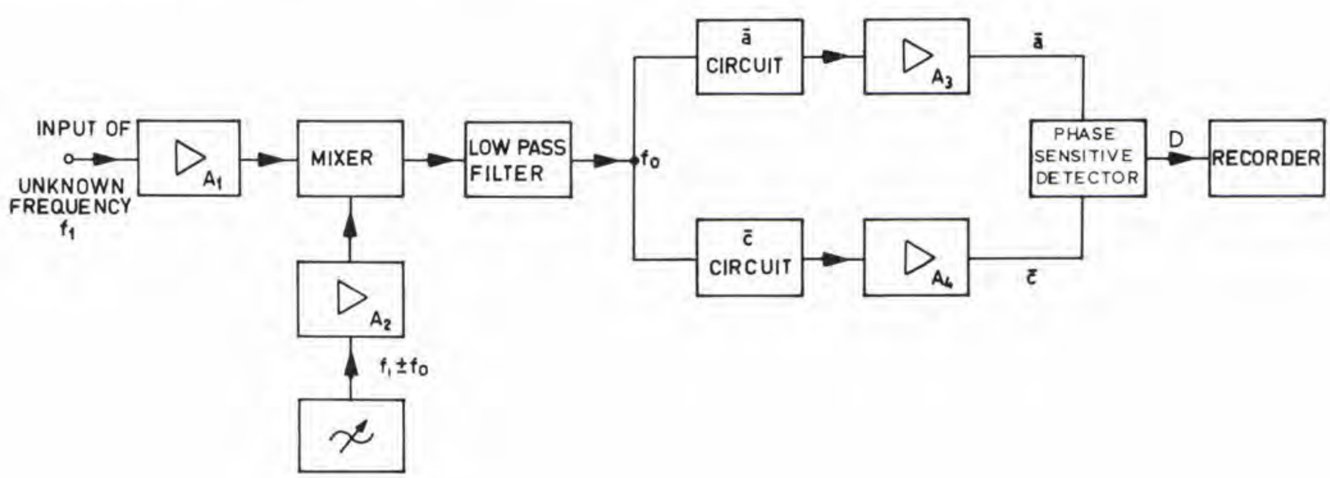

Fig. 14 Block Diagram of Complete Frequency Deviation Recorder

PART 3

SOME REALIZED CIRCUITS

3.1 Indicator with RC Networks (Fig. 15)

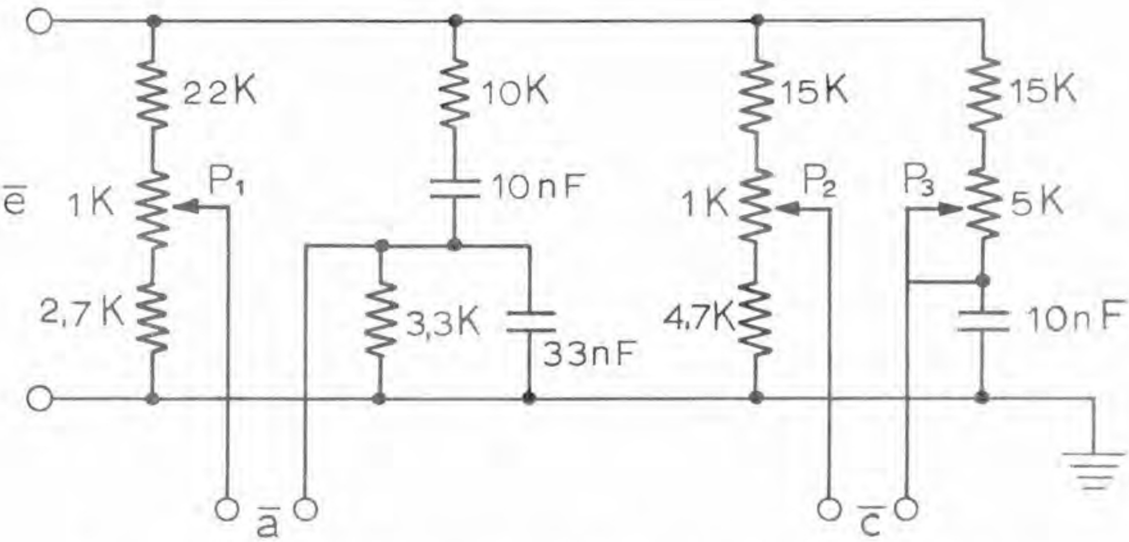

Fig. 15 Practical Circuit for RC Discriminator: f_o = 1.5 Kc

The RC Network is constructed following the principles of Figs. 2 and 6 and using Eqs. (2), (10), (35), and (36) to calculate the actual values of the resistors and condensers. The central frequency was intended to be about 1.5 kc.

The circuit has been built up with standard components with tolerances of 10%. Therefore, potentiometers are inserted on critical points:

P_1 - serves to have a complete zero for $\bar{a}$ at the frequency f_o

P_2 - brings the factor k to the right value. Eqs. (20) and (21)

P_3 - brings the factor ϵ to the right value. Eqs. (20) and (21)

P_2 and P_3 are adjusted to keep the phase difference between $\bar{a}$ and $\bar{c}$ exactly on 0 ± 180^o for all frequencies. This is a matter of repetitive correction of P_2 and P_3 at different frequencies until the final settings are found.

3.1.1 <u>Calibration.</u> This circuit has been calibrated with the $\bar{a}$-channel to the horizontal and the $\bar{c}$-channel to the vertical deflection plates of an oscilloscope. The sensitivity ratio between the two channels has been varied, and, for each ratio, the frequencies are noted for inclination angles of -45^o and $+45^o$. The results are shown in Table 1. The resultant central frequency f_o is 1555 cps.

TABLE 1

Sensitivity ratio $\frac{\bar{a}\text{-channel}}{\bar{c}\text{-channel}}$	Frequencies for inclination angles of		Frequency differences Δf_o for inclination angles of	
	-45^o	$+45^o$	-45^o	$+45^o$
500	1544	1566	- 11	+ 11
200	1527	1583	- 28	+ 28
100	1497	1612	- 58	+ 57
50	1435	1673	- 120	+ 118
20	1250	1850	- 305	+ 295
10	920	2160	- 635	+ 605
5	0	2930	-1555	+1375

3.1.2 Conclusion. It appears from Table 1 that the symmetry is excellent for relative frequency deviations Δ up to 0.2 ($\Delta f_o \lessapprox 300$ cps) and good for Δ up to 0.5 ($\Delta f_o \lessapprox 800$ cps). This is in agreement with the theoretical curve of Fig. 10. The sensitivity ratio of 500 makes an indication of 1 cps in 1600 cps clearly possible. For still higher sensitivities, the signal should be properly filtered to reduce noise and harmonics that otherwise might blur the horizontal component of the picture.

3.2 Indicator with LC-Networks (Fig. 16)

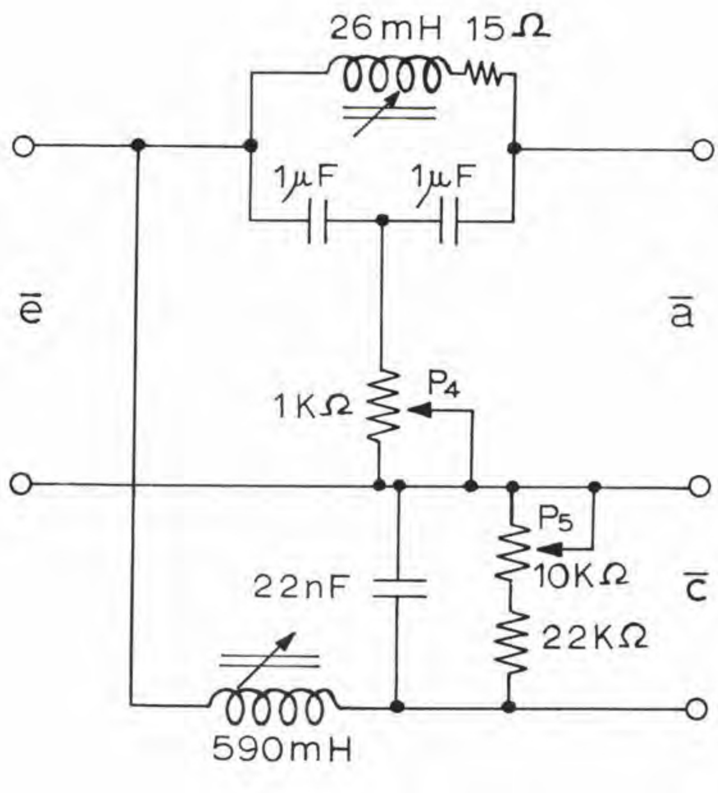

Fig. 16 Practical Circuit for LC Discriminator: f_o 1.5 Kc

This circuit is constructed from the diagrams of Figs. 4 and 5. The actual values of the components are calculated using Eqs. (5), (6), (7), (13), (14), (28), and (47). The designed central frequency was 1.4 kc.

The resistor r (Fig. 4) brings the quality factor Q_a of the Bridged-T to a value of 10. Then, the other resistor R should be 575 ohms.

According to Eq. (47), it is found

$$L_c = L_a \frac{Q_a^2 + 2}{4} = 26 \frac{102}{4} = 660 \text{ mh}$$

Then, Eq. (13) prescribes the value for C_c being 20000 pf. The nearest standard value of 22000 pf has been chosen reducing L_c to 590 mh.

Equation (28) gives the quality factor Q_c for the Phase Shifter

$$Q_c = 1/2 \; Q_a = 5$$

Then, Eq. (14) gives the value for R_c of 28.5 k ohm.

Variable resistors P_4 and P_5 have been placed in the circuit to obtain a sharp trace on the oscilloscope at all frequencies: P_4 serves to reduce $\left| \bar{a} \right|$ to zero at the frequency f_o. The circuit is regulated for all other frequencies with P_5 and the tuning lug of the 590 mh coil. This procedure requires a repeated alternative setting of coil resistor to find the combination that causes a fine trace on the screen at all frequencies.

3.2.1 Calibration. The circuit has been calibrated in the same way as described in Section 2.2.1. The central frequency was found to be 1430 cps. See Table 2.

TABLE 2

Sensitivity ratio $\frac{\bar{a}\text{-channel}}{\bar{c}\text{-channel}}$	Frequency in cps for inclination angle of		Frequency difference Δf_o in cps for inclination angles of	
	-45°	$+45^{\circ}$	-45°	$+45^{\circ}$
1000	1429.3	1430.7	- 0.7	+ 0.7
500	1428.5	1431.4	- 1.5	+ 1.4
200	1426.5	1433.4	- 3.5	+ 3.4
100	1423.0	1436.8	- 7.0	+ 6.8
50	1416.0	1443.5	-14.0	+13.5
20	1395	1464.5	-35	+34
10	1359	1499	-71	+69
5	1285	1570	-145	+140
2	1020	1760	-410	+330
1	0	2030	-1430	+600

3.2.2 Conclusion. The sensitivity of this discriminator is, for the same amplifier gain ratios, evidently about 8 times higher than that of the RC-type described in Section 2.2. This will be seen by comparing the two Eqs. (22)

and (29) concerning these two types of circuits, giving

$$\frac{\text{Eq. (22)}}{\text{Eq. (29)}} = \frac{(\epsilon - 1)^2}{\epsilon^2 + \beta^2} \approx \frac{1}{7.5}$$

since $\epsilon = \sqrt{3}$ and $\beta \approx 1$.

The experimental value of 1/8 agrees quite well with this theoretical value.

The advantage of the higher sensitivity of the LC indicator is compensated by the drawbacks inherent in coils as mentioned at the end of Section 2. 2. 2.

3. 3 Discriminator for Magnetometer

For the measurement of the changes in the earth's magnetic field, a Rubidium Vapor Magnetometer can be used. This magnetometer generates a signal with a frequency of about 210 kc which changes with the intensity of the magnetic field at the rate of 4. 66 cps per γ ($1\ \gamma = 10^{-5}$ G). A crystal oscillator converts this frequency to the frequency f_1 (Fig. 14) between 3 and 20 kc. A stable signal generator supplies the frequency $f_1 \pm f_o$.

The discriminator, which has been developed to measure the frequency deviations, will be described in detail in this section.

The center frequency f_o is 1. 5 kc, allowing a frequency deviation of 1 kc to be measured at each side. A complete circuit diagram is given in Fig. 17.

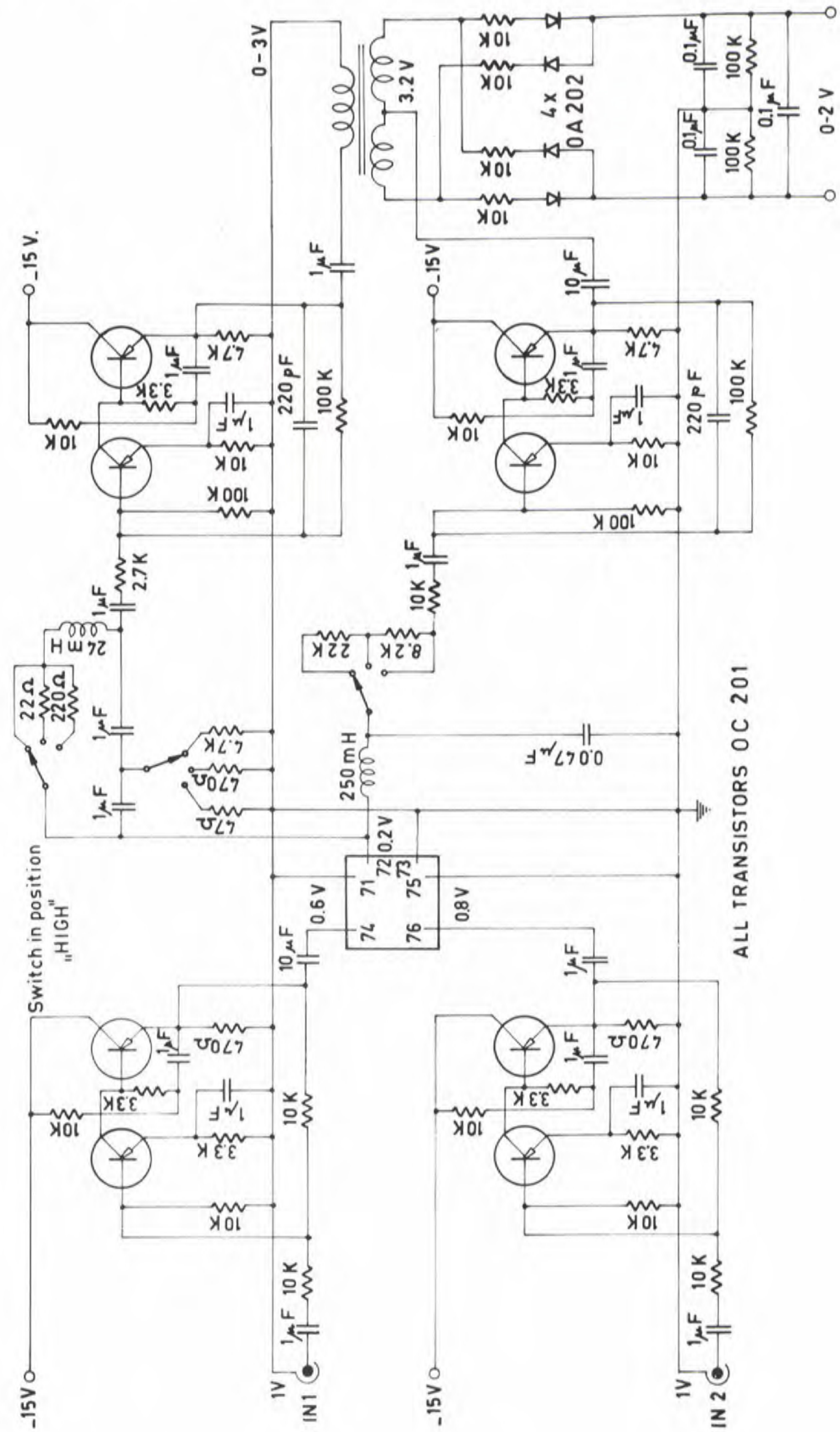

Fig. 17 Circuit Diagram of Discriminator 1500 c/s

3.3.1 The Amplifiers. The amplifiers, indicated in the block diagram in Fig. 14 as A_1 to A_4, are all the same type as described in Refs. (1) and (2). Their purpose is to drive the mixer and the detector at suitable voltage levels without loading the previous stages.

3.3.2 The Mixer. The mixer is a ready made ring modulator from "AUTELCO," "Modulator AA 22/1." (Fig. 18).

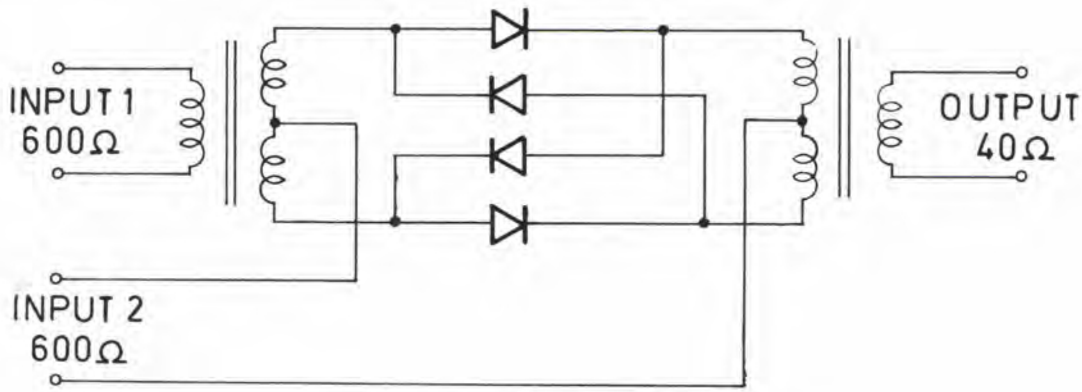

Fig. 18 "Autelco" Ring Modulator

This modulator is very well balanced; even with input frequencies of 2 and 3.5 kc, a clear 1.5 kc signal is obtained.

3.3.3 The $\bar{a}$ and $\bar{c}$-circuits. It was pointed out in Section 2.2.2 that, for a high sensitivity, the Q-factor of the Bridged-T should be high. When a lower sensitivity and a larger bandwidth is required, the Q-factor has to be reduced. Therefore, a switch is provided in the circuit to change the Q-factors to the values

$$Q_{a1} = 20 \qquad Q_{c1} = 10$$

$$Q_{a2} = 6.6 \qquad Q_{c2} = 3.3$$

$$Q_{a3} = 1.0 \qquad Q_{c3} = 0.5$$

The two condensers of the $\bar{a}$-circuit are 1 μf, giving L_a = 23 mh for a central frequency of 1500 cps.

According to Eq. (47), when $Q_a = 6.6$

$$L_c = 11\,L_a = 250 \text{ mh}$$

and the tuning capacitor in the $\bar{c}$-circuit will be 0.047 μf.

3.3.4 <u>The $\bar{c}$-Amplifier A_4</u>. Because the amplitude $\left|\bar{c}_o\right|$ at the frequency f_o is proportional to Q_c, some precaution must be taken to keep this amplitude constant. This is done by having the resistors R_c (Fig. 8) in the $\bar{c}$-circuit to take part in the feed back circuit of the amplifier A_4. As the gain of the amplifier is equal to the ratio $\frac{R\text{ feedback}}{R_c}$ this gain is inversely proportional to Q_c. See Fig. 19. As a result, the output of the amplifier A_4 at the frequency f_o is independent of Q_c.

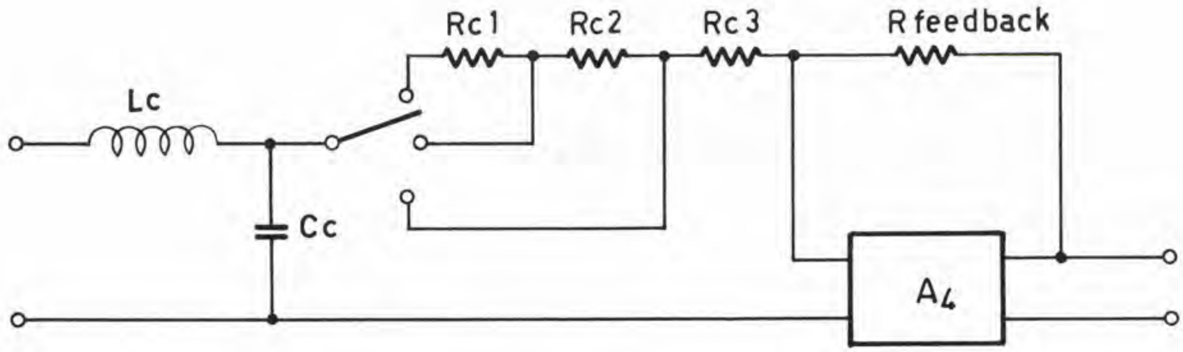

Fig. 19 Arrangement for Constant $|\bar{c}_o|$ independent of Q_c

3.3.5 The Detector. (See Fig. 11). The amplifiers, which feed the detector, are able to deliver several volts into a relatively high impedance. As the input impedance of the recorder loading the detector also is high, the detector is designed for high signal levels, using Silicon diodes OA 202 with series resistors of 10 k ohm. The RC-network is designed for a time constant of 0.03 sec.

3.3.6 Calibration. The calibration of the discriminator is performed with two signals of 1 Volt rms each; one with a frequency of 10,000 cps; the other with a variable frequency above 10 kc. It is found that the sensitivity depends on the input voltage only if this voltage is below 1 v. This is due to the limiting action of the input amplifiers and the mixer being overloaded at about 1 v.

Figures 20 and 21 give the calibration curves with the frequency difference between the two input signals as abscissae and the DC output voltage as ordinates. The curves are drawn for the three positions of the sensitivity switch: High Medium, and Low.

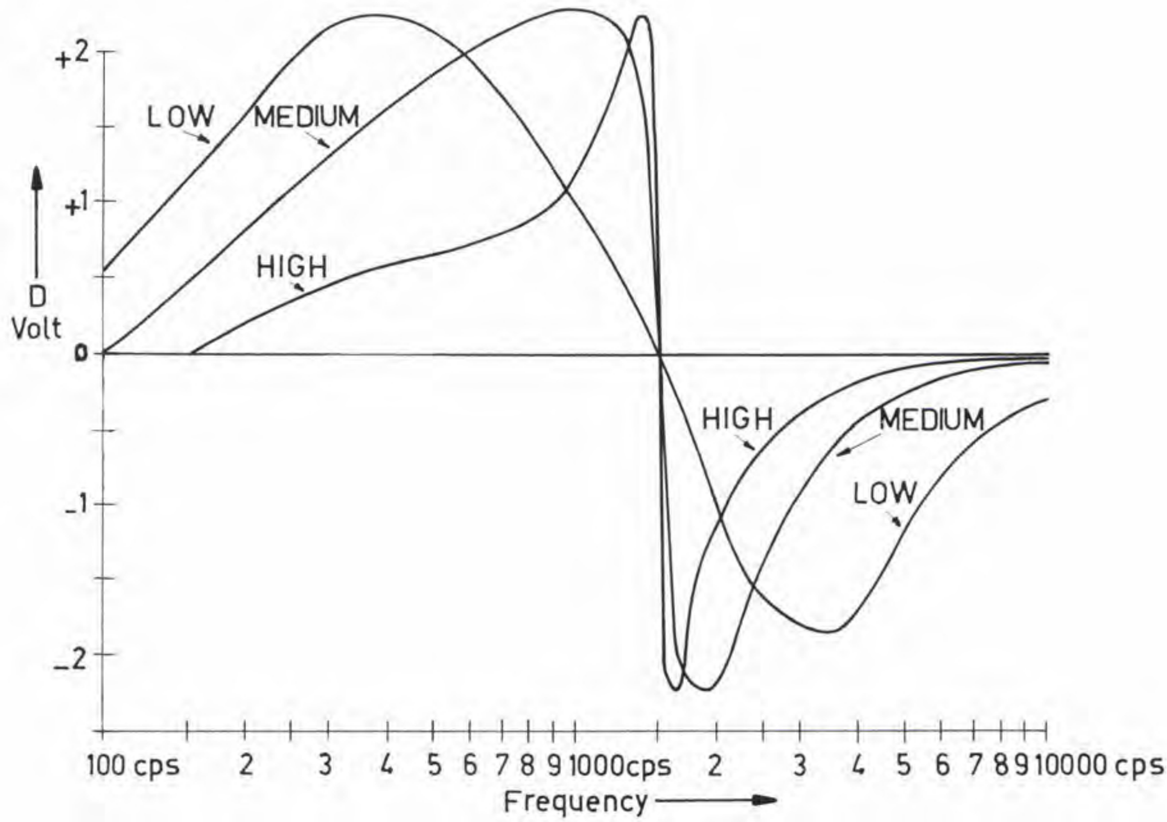

Fig. 20 Calibration Curves of Discriminator of Fig. 17

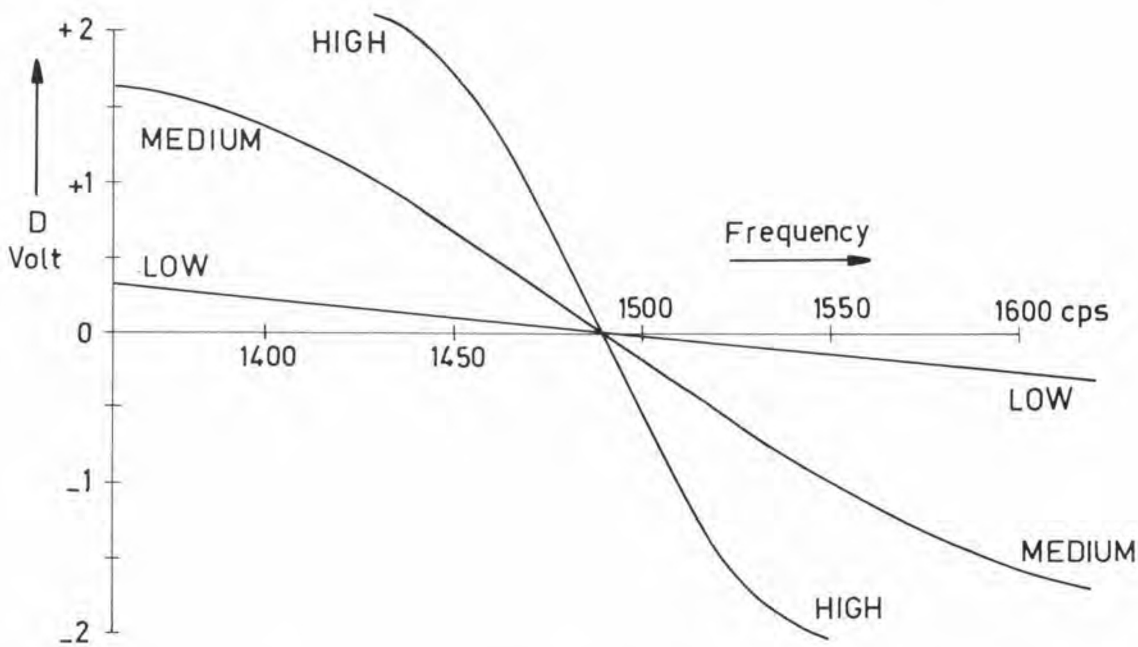

Fig. 21 Calibration Curves of Discriminator of Fig. 17

As the discriminator is intended for use with the two-channel Brush paper recorder Mark II, the conversion factors, relating the pen deflections to frequency deviations at the different sensitivities of the recorder, are given in Table 3. There is a difference in sensivitiy between the central part of the recording paper and the edges due to the non-linearity of the discriminator curves. Therefore, two factors are given in the table.

TABLE 3

DISCRIMINATOR SCALE FACTORS

SENSITIVITY		FREQUENCY SHIFT IN cps/mm	
Discriminator Switch	Brush Recorder v/mm	MIDDLE	EDGES
HIGH (20 cps/v or 50 mv/cps)	0.01	0.2	0.2
	0.02	0.4	0.4
	0.05	1.0	1.1
	0.1	2.1	3.7
	0.2	5.4	-
MEDIUM (60 cps/v or 17 mv/cps)	0.01	0.6	0.6
	0.02	1.2	1.2
	0.05	3.0	3.2
	0.1	6.2	11
	0.2	16	-
LOW (420 cps/v or 2.4 mv/cps)	0.01	4.2	4.2
	0.02	8.4	9.1
	0.05	21	29
	0.1	49	-
	0.2	120	-

At the lower sensitivities of the recorder, no full scale deflection may occur. In those cases no conversion factors are given.

The highest sensitivity allows discrimination of a frequency change of 0.2 cps, corresponding to a change in the earth's magnetic field of 0.04 γ . The lowest sensitivity allows the recording of a frequency change of about 1000 cps, corresponding to 200 γ . For larger variations of the magnetic field, the signal generator frequency has to be changed to get the mean value of the indication near to the center line of the paper strip.

3.4 Discriminator for the Sound Velocity Meter

The velocity of sound waves in sea water is measured with the aid of a Sound Velocity Meter, which generates a signal with a frequency proportional to the sound velocity. The mean frequency is about 3675 cps, with a maximum deviation of 50 cps to each side, that has to be recorded as a function of depth on a X-Y recorder with the aid of a discriminator. The block diagram of the discriminator is given in Fig. 22.

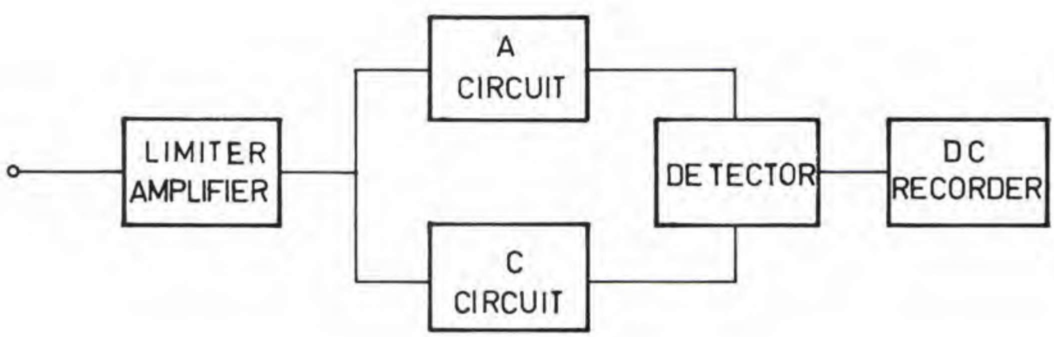

Fig. 22 Block Diagram of Sound Velocity Meter Discriminator

A complete circuit diagram is given in Fig. 23.

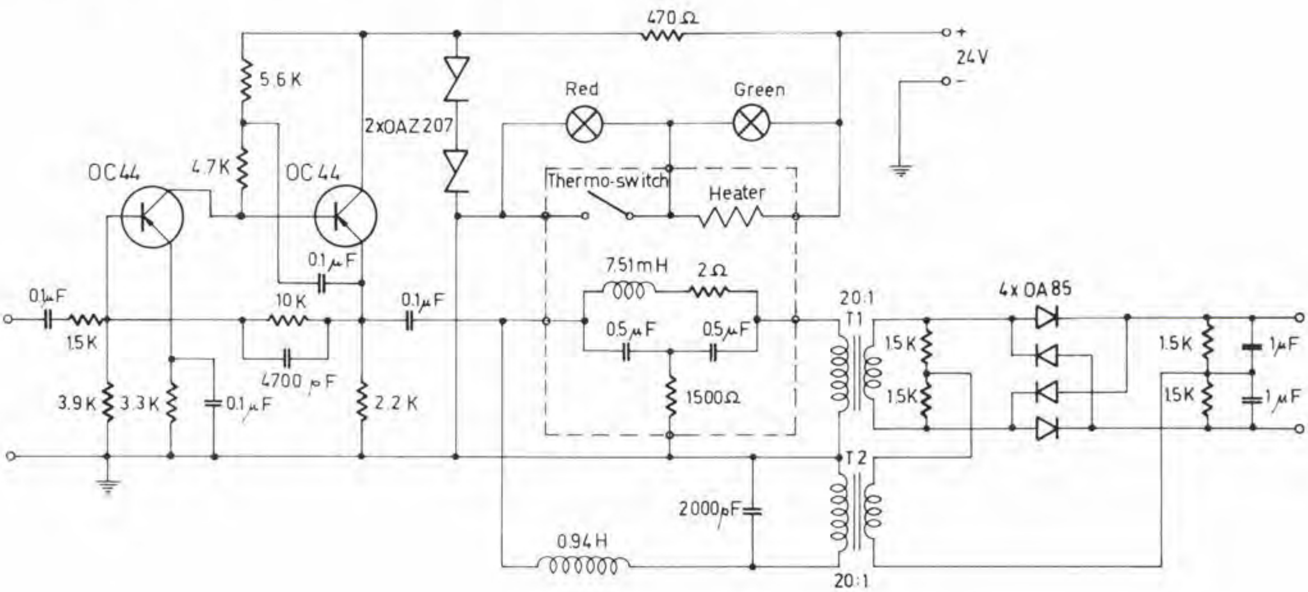

Fig. 23 Circuit Diagram of Sound Velocity Meter Discriminator

3.4.1 Limiter amplifier. The signal from the sound velocity meter is a stable square wave with a peak-to-peak value of about 4 v. As the output voltage D of the discriminator varies with the input voltage, the square wave has to be clipped. The clipping is done with an overloaded amplifier, which has a supply voltage stabilized with two Zener diodes. The influence of this limiting action is illustrated in Fig. 24, which shows the increase in sensitivity of the discriminator with increasing peak-to-peak input voltage.

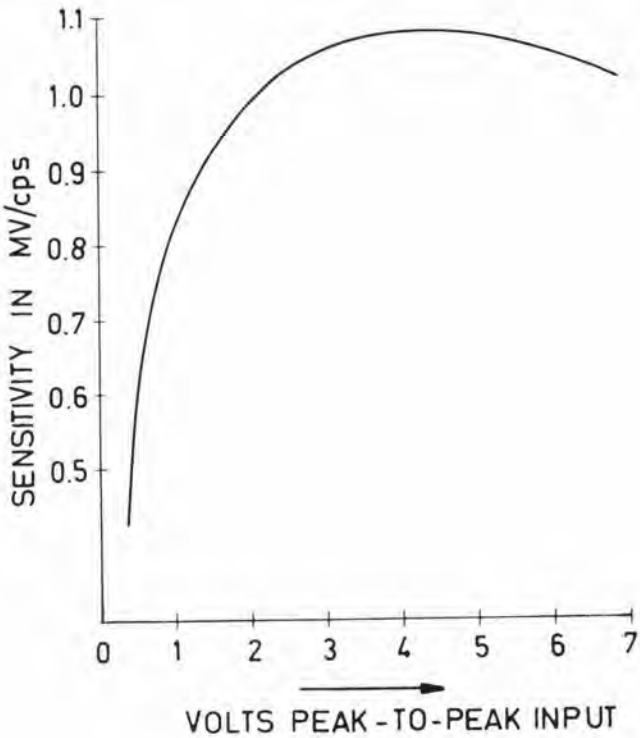

Fig. 24 Sensitivity of Discriminator as a Function of Input Signal Voltage Level

3.4.2 The $\bar{a}$-circuit. The resonant frequency of the Bridged-T circuit is 3670 cps. The Q factor is $Q_a = 34$; it is brought to this value by the additional series resistance of 2 ohms. The capacitors are Siemens Styroflex condensers 0.5 μf $\pm$ 0.3%.

3.4.3 Precision and Stability. Because one of the requirements for the discriminator is a high precision in absolute frequency indication for varying ambient temperature, the $\bar{a}$-circuit has been mounted in a thermostat oven of the type used for stabilizing precision Quartz oscillator crystals. The temperature is stabilized at 65° C $\pm$ 1°. The temperature coefficients of the different components is not known precisely, but the order of magnitude is

estimated to be:

For Styroflex capacitors

$$\frac{\Delta C}{C \cdot \Delta T} \approx - 150.10^{-6} \quad /^{\circ}C$$

For Siemens Siferrit 550 M25 with a $\mu_g = 50$

$$\frac{\Delta L}{L \cdot \Delta T} \approx + 100.10^{-6} \quad /^{\circ}C$$

The temperature coefficient of the resonant frequency will be found from $\omega^2 LC = 1$ to be

$$\frac{\Delta f}{f \cdot \Delta T} = - \frac{1}{2} \quad \frac{\Delta C}{C \Delta T} - \frac{1}{2} \quad \frac{\Delta L}{L \cdot \Delta T}$$

$$= 75.10^{-6} - 50.10^{-6} = 25.10^{-6} \quad /^{\circ}C$$

when $f_o = 3670$ cps,

$$\frac{\Delta f}{\Delta T} = 0.1 \text{ cps} \quad /^{\circ}C^*$$

---

*A change in the central frequency f_o of 8 cps was measured when the temperature changed from 20° C to 60°C, giving a temperature coefficient of

$$\frac{\Delta f}{\Delta T} = \frac{8}{40} = 0.2 \text{ cps} \quad /^{\circ}C$$

3.4.4 The $\bar{c}$-circuit. According to Eq. (47) the inductance L_c should be

$$L_c = L_a \frac{Q_a^2 + 2}{4}$$

With $L_a = 7.5$ mh and $Q_a = 34$ it is found that $L_c = 2.2$ h

However, it appears that the load resistance R_c (Fig. 13) would be an impractically high value. In the design of this discriminator, the resistor R_c is incorporated in the load introduced by the transformer T2 and the rectifier bridge (Fig. 23). R_c was found to be about 400 k ohm.

The values of C_o and L_c are determined from Eqs. (13) and (14) when Q_c, ω_o and R_c are given. With $Q_c = 17$ and $R_c \approx 400$ k ohm it is found that

$$C_c = 2000 \text{ pf}$$

$$L_c = 0.94 \text{ h}$$

3.4.5 The Rectifier. Because of the high sensitivity of the recorder, the output voltage D should be of the order of magnitude of 10 mv. Therefore, the levels of $\bar{a}$ and $\bar{c}$ are stepped down by the transformers T_1 and T_2 by a factor 20, unloading the $\bar{a}$ and $\bar{c}$-circuits from the impedance of the rectifier by a factor 400.

Because of the low signal levels, the diodes are of the germanium type, OA 85, and the load resistances are low, 1.5 k ohm, giving with the 1 μF a condensers time constant of 1.5 ms.

3.4.6 Calibration. The discriminator has been calibrated with a square wave signal of a 4 v peak-to-peak. Figure 25 gives the DC output voltage in millivolts versus the signal frequency.

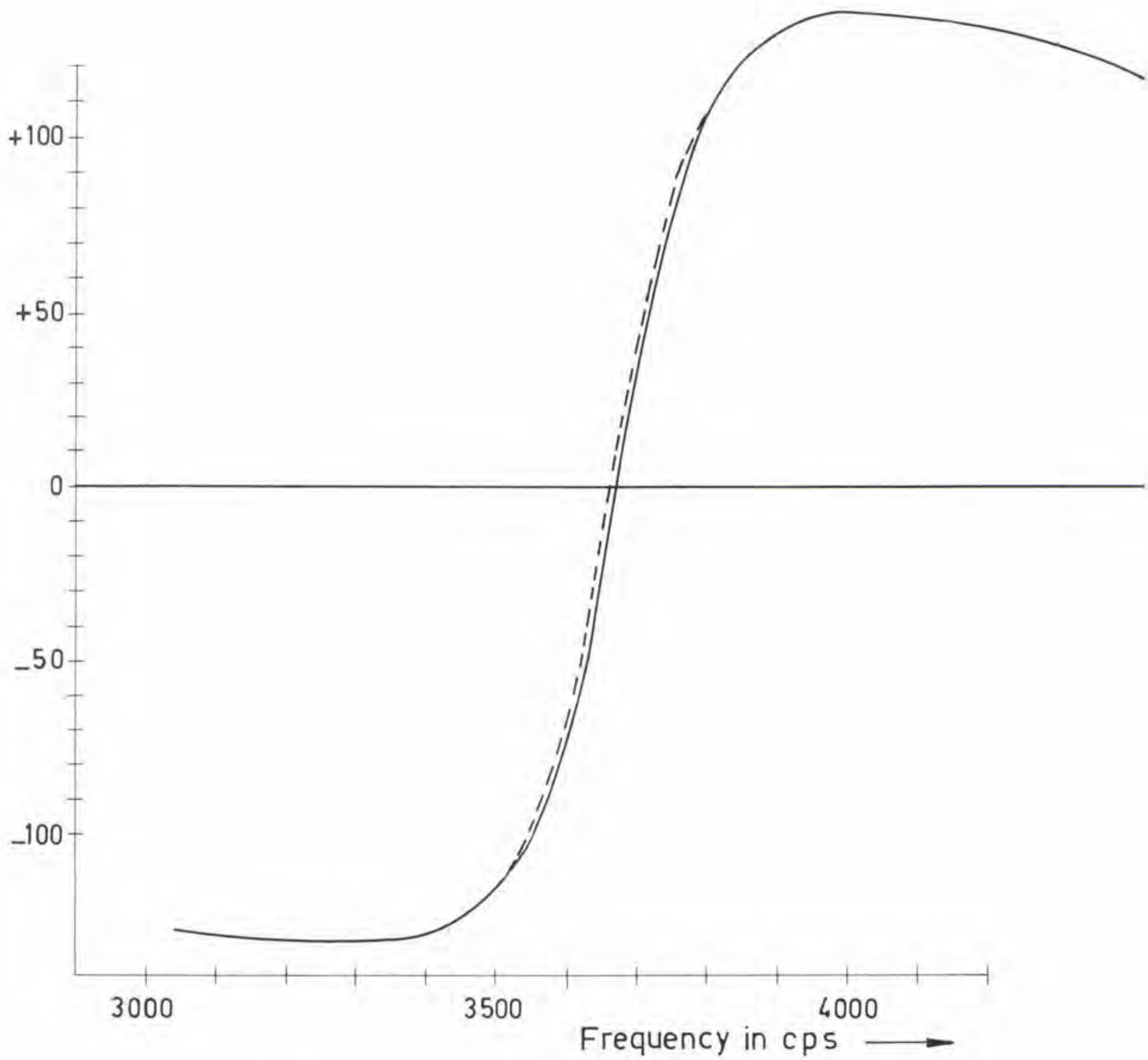

Fig. 25 Calibration Curve of Discriminator of Fig. 23

Figure 26 is an enlargement of the central, most important, part of the curve of Fig. 25.

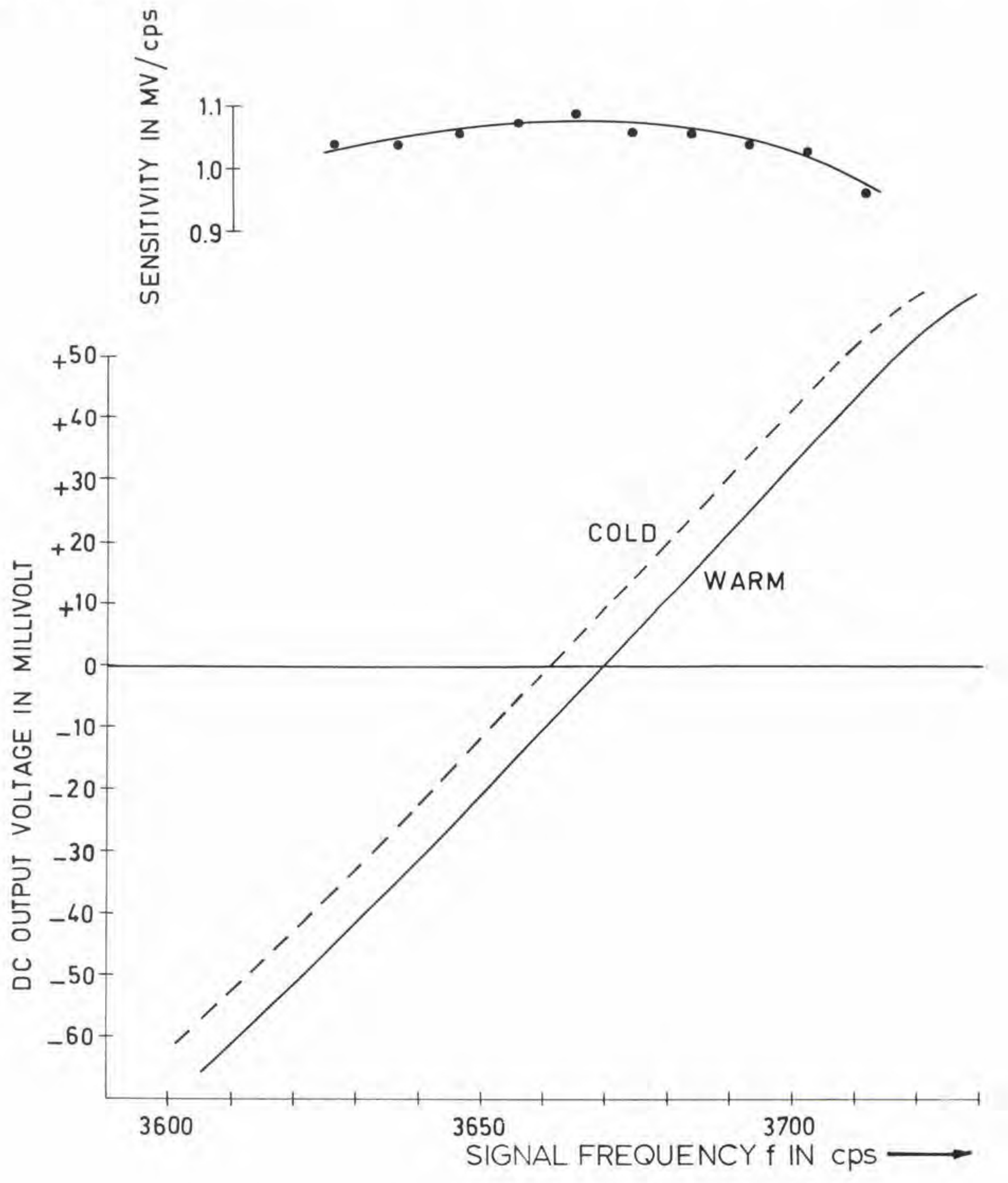

Fig. 26 Calibration Curve of Discriminator of Fig. 23

The dotted lines refer to normal room temperature: discriminator "cold." The full drawn curve is valid after an oven warm-up time of at least one hour: discriminator "warm," temperature 65^{o}C. The sensitivity of the discriminator has been accurately measured with a frequency counter, giving the frequency with the precision of 0.1 cps.

At the top of Fig. 26, the curve for the sensitivity versus frequency is given in millivolts per cycles per second frequency change. At the central frequency 3670 cps the sensitivity is maximum:

$$S_{Do} = 1.07 \text{ mv/cps}$$

slowly decreasing at both ends of the frequency range.

3.4.7 Conclusions.

1. The linearity of the discriminator curve in Fig. 26 appears to be reasonably good within the desired frequency range between 3620 and 3720 cps.

2. The short term stability gives a reproducible indication for one day within 0.3 cps, giving a precision of 10^{-4}.

3. The long term stability is not well known. A difference in f_o of 1 cps has been found between one day and the next, reducing the precision to 3.10^{-4}. However, the difference may be due to an aging effect of the styroflex condensers in the $\bar{a}$-circuit. These condensers have a maximum working temperature of 70^{o}C; they are heated each day from 15^{o}C to 65^{o}C, causing some thermal deformation. Shortly after the construction of the discriminator, there was a daily increase of f_o of

about 5 cps that decreased gradually to 1 cps per day. It may be, finally, that a stable situation has been reached.

4. The sensitivity of the instrument allows a discrimination of 0.1 cps, provided the recorder indicates a difference in DC voltage of 0.1 mv.

APPENDIX I

Derivation of the Equations.

Equation (3)

(1) and (2) $\omega R_1 C_1 = \beta$

Figure 2: $$\frac{\bar{a}}{\bar{e}} = \frac{j \beta n}{1 - \beta^2 + j \beta (n+2)} - \frac{n}{n+2}$$

$$= \frac{n}{n+2} \cdot \frac{\beta^2 - 1}{1 - \beta^2 + j \beta (n+2)}$$

$$= \frac{n}{n+2} \cdot \frac{1}{-1 + j \frac{\beta}{\beta^2 - 1} (n+2)} \qquad (3)$$

Equation (12)

(1) and (10) $\omega R_3 C_3 = \epsilon \beta$

Figure 6: $$\frac{\bar{c}}{\bar{e}} = \frac{1}{1 + j \epsilon \beta} - k \tag{11}$$

$$= \frac{1 - k (1 + \epsilon^2 \beta^2) - j \epsilon \beta}{1 + \epsilon^2 \beta^2}$$

$$\mathrm{tg}\ \gamma = \frac{- \epsilon \beta}{1 - k (1 + \epsilon^2 \beta^2)} \tag{12}$$

Equation (15)

(1) and (13) $$\omega^2 L_c C_c = \beta^2$$

(1), (13), and (14) $$\frac{\omega L_c}{R_c} = \frac{\beta}{Q_c}$$

Figure 8: $$\frac{\bar{c}}{\bar{e}} = \frac{1}{1 - \beta^2 + j \frac{\beta}{Q_c}} \tag{15}$$

Equations (20) and (21)

(19) $$(n+2) \frac{\beta}{\beta^2 - 1} = \frac{\epsilon \beta}{k (1 + \epsilon^2 \beta^2) - 1}$$

$$(n+2)\left[k\,(1+\epsilon^2\beta^2)-1\right]=\epsilon\,(\beta^2-1) \tag{19a}$$

$$\beta=1 \rightarrow (n+2)\left[k\,(1+\epsilon^2)-1\right]=0$$

$$k\,(1+\epsilon^2)=1$$

$$k=\frac{1}{\epsilon^2+1} \tag{21}$$

$$1-k=\frac{\epsilon^2}{\epsilon^2+1} \tag{21a}$$

(19a) $\beta=0 \rightarrow (n+2)\,(k-1)=-\epsilon$

(21a) $(n+2)\,\dfrac{\epsilon^2}{\epsilon^2+1}=\epsilon$

$$n+2=\frac{\epsilon^2+1}{\epsilon}$$

$$n=\frac{(\epsilon-1)^2}{\epsilon} \tag{20}$$

<u>Equation (22)</u>

(20) $n=\dfrac{(\epsilon-1)^2}{\epsilon}$

(21) $k=\dfrac{1}{\epsilon^2+1}$

(3) $$\frac{\bar{a}}{\bar{e}} = \frac{n}{n+2} \cdot \frac{-1}{1 - j\,\frac{\beta}{\beta^2 - 1}\,(n+2)}$$

(11) $$\frac{\bar{c}}{\bar{e}} = \frac{1}{1 + j\,\epsilon\,\beta} - k$$

Substitution of (20) in (3) gives

$$\frac{\bar{a}}{\bar{e}} = \frac{\epsilon\,(\epsilon - 1)^2}{\epsilon^2 + 1} \cdot \frac{\beta^2 - 1}{\epsilon\,(1 - \beta^2) + j\,\beta\,(\epsilon^2 + 1)} \qquad (3a)$$

Substitution of (21) in (11) gives

$$\frac{\bar{c}}{\bar{e}} = \frac{\epsilon}{\epsilon^2 + 1} \cdot \frac{\epsilon\,(1 - \beta^2) - j\,\beta\,(\epsilon^2 + 1)}{\epsilon^2\ \beta^2 + 1} \qquad (11a)$$

(18) $$\mathrm{tg}\,\phi = \frac{\bar{a}}{\bar{c}}$$

Substitution of (3a) and (11a) in (18) gives

$$\mathrm{tg}\,\phi = (\epsilon - 1)^2 \ \frac{(\beta^2 - 1)\ (\epsilon^2\,\beta^2 + 1)}{\epsilon^2(1 - \beta^2)^2 + \beta^2\,(\epsilon^2 + 1)^2}$$

$$= \frac{(\epsilon - 1)^2\ (\beta^2 - 1)}{\epsilon^2 + \beta^2} \qquad (22)$$

Equations (24) and (25)

$$\frac{2}{Q} \cdot \frac{\beta}{\beta^2 - 1} = \frac{\epsilon \beta}{k(1 + \epsilon^2 \beta^2) - 1} \tag{23}$$

$$2k + 2k\epsilon^2\beta^2 - 2 = Q\epsilon\beta^2 - \epsilon Q \tag{23a}$$

$$\beta = 1 \rightarrow 2k + 2k\epsilon^2 - 2 = 0$$

$$k = \frac{1}{\epsilon^2 + 1} \tag{25}$$

$$1 - k = \frac{\epsilon^2}{\epsilon^2 + 1} \tag{25a}$$

(23a) $$\beta = 0 \rightarrow 2k - 2 = -\epsilon Q$$

$$1 - k = \frac{\epsilon Q}{2}$$

(25a) $$\frac{\epsilon^2}{\epsilon^2 + 1} = \frac{\epsilon Q}{2}$$

$$Q = \frac{2\epsilon}{\epsilon^2 + 1} \tag{24}$$

Equation (26)

$$(8) \qquad \frac{\bar{a}}{\bar{e}} = \frac{1}{1 - j \dfrac{\beta}{\beta^2 - 1} \cdot \dfrac{2}{Q_a}}$$

$$(11) \qquad \frac{\bar{c}}{\bar{e}} = \frac{1}{1 + j \epsilon \beta} - k$$

Substitute (24) in (8):

$$\frac{\bar{a}}{\bar{e}} = \frac{\epsilon (\beta^2 - 1)}{\epsilon (\beta^2 - 1) - j \beta (\epsilon^2 + 1)} \qquad (8a)$$

Substitute (25) in (11):

$$\frac{\bar{c}}{\bar{e}} = \frac{\epsilon}{\epsilon^2 + 1} \cdot \frac{\epsilon (1 - \beta^2) - j \beta (\epsilon^2 + 1)}{\epsilon^2 \beta^2 + 1} \qquad (11a)$$

Substitute (8a) and (11a) in (18):

$$\mathrm{tg}\ \phi = \frac{(\epsilon^2 + 1)(\epsilon^2 \beta^2 + 1)(\beta^2 - 1)}{\epsilon^2 (\beta^2 - 1)^2 + \beta^2 (\epsilon^2 + 1)^2}$$

$$= \frac{(\epsilon^2 + 1)(\beta^2 - 1)}{\epsilon^2 + \beta^2} \qquad (26)$$

Equation (29)

(8) $$\frac{\bar{a}}{\bar{e}} = \frac{1}{1 - j \dfrac{\beta}{\beta^2 - 1} \cdot \dfrac{2}{Q_a}}$$

(15) $$\frac{\bar{c}}{\bar{e}} = \frac{1}{1 - \beta^2 + j \dfrac{\beta}{Q_c}}$$

(18) $\longrightarrow$ $$\text{tg}\,\phi = \frac{(\beta^2 - 1)\left(1 - \beta^2 + j \dfrac{\beta}{Q_c}\right)}{(\beta^2 - 1 - j\beta \dfrac{2}{Q_a})}$$

with (28) $$Q_a = 2\,Q_c$$

$$\text{tg}\,\phi = 1 - \beta^2 \qquad (29)$$

Equation (34)

Frequency dependent part of (22) and (26):

$$\text{tg}\,\phi = \frac{\beta^2 - 1}{\beta^2 + \epsilon^2}$$

(32) $$\beta = 1 + \Delta$$

$$\beta^2 = 1 + 2\Delta + \Delta^2$$

$$\mathrm{tg}\,\phi = \frac{\Delta^2 + 2\Delta}{1 + 2\Delta + \Delta^2 + \epsilon^2}$$

(33) $$\longrightarrow \frac{\Delta^2 + 2\Delta}{1 + 2\Delta + \Delta^2 + \epsilon^2} = -\frac{\Delta^2 - 2\Delta}{1 - 2\Delta + \Delta^2 + \epsilon^2}$$

$$(\Delta + 2)(\epsilon^2 + 1 - 2\Delta + \Delta^2) = (2 - \Delta)(\epsilon^2 + 1 + 2\Delta + \Delta^2)$$

There are two solutions: $\Delta = 0$ and $\Delta^2 = 3 - \epsilon^2$

Taking the last one: $\epsilon^2 = 3 - \Delta^2$

Equation (43)

(3) $$\frac{\bar{a}}{\bar{e}} = \frac{n}{n+2} \cdot \frac{-1}{1 - j\,\frac{\beta}{\beta^2 - 1}(n+2)}$$

(32) $$\beta = 1 + \Delta$$

$$\beta^2 - 1 = \Delta(2 + \Delta)$$

$$\left(\frac{\beta}{\beta^2 - 1}\right)_{\Delta \to 0} = \frac{1 + \Delta}{\Delta\,(2 + \Delta)} \longrightarrow \frac{1}{2\,\Delta}$$

(3) $$\left(\frac{\bar{a}}{\bar{e}}\right)_{\Delta \to 0} = \frac{n}{n + 2} \cdot \frac{-1}{1 - j\,\frac{n + 2}{2\,\Delta}}$$

$$= \frac{n}{n + 2} \cdot \frac{-2\,j\,\Delta}{n + 2}$$

$$= -\,\frac{2\,jn\,\Delta}{(n + 2)^2}$$

(42) $$S_o = \left|\frac{\bar{a}}{\Delta}\right|_{\bar{e}\,=\,1\text{ Volt}}$$

$$= \frac{2n}{(n + 2)^2} \qquad (43)$$

Equation (44)

(8) $$\frac{\bar{a}}{\bar{e}} = \frac{1}{1 - j\,\frac{\beta}{\beta^2 - 1} \cdot \frac{2}{Q_a}}$$

$\beta \to 1$ or $\Delta \to 0$ gives $\frac{\beta}{\beta^2 - 1} \longrightarrow \frac{1}{2\,\Delta}$

$$\left(\frac{\bar{a}}{\bar{e}} \right)_{\Delta \to 0} = \frac{1}{1 - \frac{j}{\Delta Q_a}}$$

$$= j \Delta Q_a$$

(42) $$\longrightarrow S_o = Q_a \tag{44}$$

DISTRIBUTION LIST

Minister of Defense Brussels, Belgium	10 copies
Minister of National Defense Department of National Defense Ottawa, Canada	10 copies
Chief of Defense, Denmark Kastellet Copenhagen Ø, Denmark	10 copies
Minister of National Defense Division Transmissione-Ecoute-Radar 51 Latour Maubourg Paris 7^e^, France	10 copies
Minister of Defense Federal Republic of Germany Bonn, Germany	10 copies
Minister of Defense Athens, Greece	10 copies
Ministry of National Defense Navy General Staff Rome, Italy	10 copies
Minister of National Defense Plein 4, The Hague, Netherlands	10 copies
Minister of National Defense Storgaten 33, Oslo, Norway	10 copies
Minister of National Defense, Portugal Care Portuguese Military Attaché 3 Rue Noisiel Paris, France	10 copies
Minister of National Defense Ankara, Turkey	10 copies
Minister of Defense London, England	18 copies
Supreme Allied Commander Atlantic (SACLANT) Norfolk 11, Virginia	5 copies
SACLANT Representative in Europe (SACLANTREPEUR) Place du Marechal de Lattre de Tassigny Paris 16^{e}, France	1 copy
Commander in Chief Western Atlantic Area (CINCWESTLANT) Norfolk 11, Virginia	1 copy
Commander in Chief Eastern Atlantic Area (CINCEASTLANT) Eastbury Park, Northwood Middlesex, England	1 copy
Maritime Air Commander Eastern Atlantic Area (COMAIREASTLANT) R.A.F. Northwood Middlesex, England	1 copy
Commander Submarine Force Eastern Atlantic (COMSUBEASTLANT) Fort Blockhouse Gosport, Hants, England	1 copy
Commander, Canadian Atlantic (COMCANLANT) H.M.C. Dockyard Halifax, Nova Scotia	1 copy
Commander Ocean Sub-Area (COMOCEANLANT) Norfolk 11, Virginia	1 copy
Supreme Allied Commander Europe (SACEUR) Paris, France	7 copies
SHAPE Air Defence Technical Center P.O. Box 174 Stadhouders Plantsoen 15 The Hague, Netherlands	1 copy
Allied Commander in Chief Channel (CINCCHAN) Fort Southwick, Fareham Hampshire, England	1 copy
Commander Allied Maritime Air Force Channel (COMAIRCHAN) Northwood, England	1 copy
Commander in Chief Allied Forces Mediterranean (CINCAFMED) Malta, G.C.	1 copy
Commander South East Mediterranean (COMEDSOUEAST) Malta, G.C.	1 copy

Commander Central Mediterranean
(COMEDCENT)
Naples, Italy — 1 copy

Commander Submarine Mediterranean
(COMSUBMED)
Malta, G.C. — 1 copy

National Liaison Representatives

NLR Belgium
Belgian Military Mission
3330 Garfield Street, N.W.
Washington, D.C. — 1 copy

NLR Canada
Canadian Joint Staff
2450 Massachusetts Avenue, N.W.
Washington, D.C. — 1 copy

NLR Denmark
Danish Military Mission
3200 Whitehaven Street, N.W.
Washington, D.C. — 1 copy

NLR France
French Military Mission
1759 "R" Street, N.W.
Washington, D.C. — 1 copy

NLR Germany
German Military Mission
3215 Cathedral Avenue, N.W.
Washington, D.C. — 1 copy

NLR Greece
Greek Military Mission
2228 Massachusetts Avenue, N.W.
Washington, D.C. — 1 copy

NLR Italy
Italian Military Mission
3221 Garfield Street, N.W.
Washington, D.C. — 1 copy

NLR Netherlands
Netherlands Joint Staff Mission
1470 Euclid Street, N.W.
Washington, D.C. — 1 copy

NLR Norway
Norwegian Military Mission
2720 34th Street, N.W.
Washington, D.C. — 1 copy

NLR Portugal
Portuguese Military Mission
2310 Tracy Place, N.W.
Washington, D.C. — 1 copy

NLR Turkey
Turkish Joint Staff Mission
2125 LeRoy Place, N.W.
Washington, D.C. — 1 copy

NLR United Kingdom
British Defence Staffs, Washington
3100 Massachusetts Avenue, N.W.
Washington, D.C. — 1 copy

NLR United States
SACLANT
Norfolk 11, Virginia — 40 copies

Scientific Committee of National Representatives

Dr. J.E. Keyston
Defense Research Board
Department of National Defense
Ottawa, Canada — 1 copy

G. Meunier
Ingenieur en Chef des Genie Maritime
Services Technique des Constructions et Armes Navales
8 Boulevard Victor
Paris 15^{e}, France — 1 copy

Dr. E. Schulze
Bundesministerium der Verteidigung
ABT H ROMAN 2/3
Bonn, Germany — 1 copy

Commander A. Pettas
Ministry of National Defense
Athens, Greece — 1 copy

Professor Dr. Maurizio Federici
c/o MARICOMITARMI
Ministero della Marina
Rome, Italy — 1 copy

Dr. M.W. Van Batenburg
Physisch Laboratorium RVO-TNO
Waalsdorpvlakte
The Hague, Netherlands — 1 copy

Mr. A.W. Ross
Department of Physical Research
Admiralty, Whitehall
London S.W. 1, England — 1 copy

Dr. J.E. Henderson
Department of Physics
University of Washington
Seattle 5, Washington — 1 copy

....

Standing Group, NATO
(SGN)
Room 2C256, The Pentagon
Washington 25, D.C. — 3 copies

Standing Group Representative
(SGREP)
Place du Marechal de Lattre de Tassigny
Paris 16^{e}, France — 5 copies